



## Procedia Computer Science

Volume 66, 2015, Pages 122-131



YSC 2015. 4th International Young Scientists Conference on Computational Science

# FEM hydroelastic models with application to the nonlinear response of large floating bodies in shallow wave conditions

## Angeliki E. Karperaki<sup>1</sup>

<sup>1</sup>School of Naval Architecture and Marine Engineering, National Technical University of Athens, Athens, Greece karperaki.ang@gmail.com

#### **Abstract**

A higher order finite element scheme is presented for the study of the transient hydroelastic response of a floating, thin, nonlinear strip in shallow wave conditions. First, nonlinear effects are introduced only in the elasticity model, where large deflections and non-negligible normal stress variation in the lateral direction are assumed. The nonlinear beam is initially coupled with the linearized and subsequently with the full nonlinear Shallow Water equations, introducing nonlinearity in both the hydrodynamics and the elasticity model. The effects of the incorporated nonlinear effects are assessed through a numerical example featuring an elevation pulse of increasing steepness.

Keywords: transient hydroelasticity, large floating bodies, Shallow Water Equations, Galerkin FEM, nonlinear floating elastic strip

#### 1 Introduction

The study of the hydroelastic interaction between ocean waves and large floating bodies is highly relevant to both marine engineering and polar science (Squire, 2008). Geophysical formations and pontoon-type Very Large Floating Structures (or VLFS) exhibit large horizontal dimensions compared to thickness. Due to their slenderness, hydroelastic effects are dominant over rigid body motion (Wang, Watanabe, & Utsunomiya, 2008). The majority of works on hydroelasticity consider the response of a thin, floating body in the frequency domain where eigenfunction expansion methods, Galerkin schemes and Green functions have been used (Chen, Wu, Cui, & Juncher Jensen, 2006). In order to account for irregular forcing however, transient analysis tools, like direct time integration schemes and Fourier transforms need to be employed. Some contributions in the study of the transient hydroelastic response of a floating strip include those of Papathanasiou *et al.* (2015 (a)), (2015 (b)) and Sturova *et al.* (2010). In the literature, floating bodies are most commonly modeled as thin plates under the Kirchhoff-Love assumptions ( (Meylan & Squire, 1994), (Sturova, A., Fedotova, Chubarov, & Komarov, 2010),

(Papathanasiou T., Karperaki, Theotokoglou, & Belibassakis, 2015 (b))). However, several attempts have been made to include higher order elasticity models like the Reissner-Mindlin or the Von Karman plates (Chen, Juncher Jensen, Cui, & Fu, 2003). For the hydrodynamic modeling, small amplitude wave theory is most commonly used. Special attention is paid in shallow water models, since a variety of engineering applications positions floating structures nearshore, making shallow and variable bathymetry effects crucial. For the hydroelastic response of large floating bodies over general bathymetry, modelled as thin elastic plates, a coupled-mode system has been derived in Belibassakis and Athanassoulis in (2005) and Belibassakis and Athanassoulis (2006). This method is based on a local vertical expansion of the wave potential in terms of hydroelastic eigenmodes, extending earlier approaches for the propagation of water waves in variable bathymetry regions (Athanassoulis & Belibassakis, 1999).

Several attempts have been made to study the dynamic response of floating plates within the scope of shallow water models; notably in Sturova *et al.* (2010) the linear plate is coupled with two Boussinesq-type models, and the Green-Naghdi equations, while in Hegarty and Squire (2004) nonlinear models are developed for the study of the hydroealstic interaction between large amplitude ocean waves and a thin ice floe. In this latter work, nonlinear terms are introduced in both the equations for the fluid and the plate model.

In the present contribution, the finite element method is employed for the solution of the transient 1D hydroelastic problem over variable, shallow bathymetry. At first, nonlinear effects are incorporated in the simplified elasticity model, while the linearized shallow water equations are employed for the hydrodynamic modeling. Considering large deflections and non-negligible lateral stress variation, the nonlinear beam introduced by Gao (1996), is considered. Next, nonlinearity is also incorporated in the hydrodynamic modeling through the employment of the full Shallow Water equations. The derived nonlinear models are compared against the Euler-Bernoulli floating beam model presented in Papathanasiou *et al.* (2015 (b))

In Sect. 2, after presenting the governing equations and the aforementioned nonlinear models, the corresponding initial-boundary value (IBV) hydroelastic problems are defined. Subsequently, in Sect. 3 the variational equivalent of the IBV problems will be derived, while the higher-order finite element scheme used for the solution of these problems is presented. In Sect. 4 the solutions given by the nonlinear models are examined in a numerical example featuring variable bathymetry. Different excitation steepness values are considered in order to examine the dominance of the incorporated nonlinear terms.

## 2 Governing Equations

In the present section the mathematical formulation of the 1D hydroelastic model is presented. Consider a layer of inviscid and irrotational fluid of density  $\rho_w$ , confined in the domain  $\Omega$  (see Figure 1) in the xz plane. The domain is decomposed into three regions, namely  $\Omega_1 \equiv (-\infty,0)$ ,  $\Omega_0 \equiv (0,L)$  and  $\Omega_2 \equiv (L,\infty)$ , where L is the length of the strip. Due to the fluid assumptions, a velocity potential function  $\phi$  can be defined as  $u = \partial_x \phi$  where u denotes the horizontal fluid velocity. The floating plate is assumed to extend infinitely in the y direction, vertical to the page, corresponding to a beam under normal incident wave loading. The beam deflection and the fluid upper surface elevation are assumed to coincide at all times. Additionally, the floating strip features uniform thickness  $\tau$  and density  $\rho_e$ . The bathymetry function is given as b(x) = h(x) - d, where h(x) is the local depth and  $d = \rho_w^{-1} \rho_e \tau$  is the plate draft, which is non-zero only at the region of the hydroelastic coupling. At the free water surface regions, the Shallow Water Equations (SWE) are considered,

$$\partial_{t}u + u\partial_{x}u + g\partial_{x}\eta = 0, \tag{1}$$

$$\partial_{t} \eta + \partial_{x} \left( [b(x) + \eta] \partial_{x} \phi \right) = 0 \tag{2}$$

With the added assumption of small steepness waves, the linearised Shallow Water Equations (LSWE) are straightforwardly derived by excluding the nonlinear terms in Eqs. (1) and (2). In the hydroelasticity dominated region the coupling is accomplished through the dynamic pressure applied at the floating strip, given by

$$p = \rho_{w}g\eta + \rho_{w}\partial_{t}\phi + \frac{\rho_{w}}{2}(\partial_{x}\phi)^{2}$$
(3)

For the floating body, the nonlinear elastic beam model introduced by Gao (Gao, 1996) will be examined in the following analysis, while the floating Euler-Bernoulli beam (EB) will provide a linear benchmark solution. In the classical beam theory, the deflection of a thin, elastic and homogeneous floating body under vertical loading, denoted by q(x,t), and pressure forcing given by the linearized Eq. (3), is given by

$$m\partial_t^2 \eta + D\partial_v^4 \eta + \rho_w g \eta + \rho_w \partial_t \phi = -q(x,t) \tag{4}$$

The fully linear EB-LSW model, presented in Papathanasiou *et al.* (2015 (b)) will provide the basis for the assessment of the incorporated nonlineariaty. The first term (LHS) in Eq. (4) accounts for inertial effects, where m is the mass per unit length of the floating body, while the second term accounts for flexural effects and D denotes the bending rigidity of the beam. The Gao beam (GB) model (Gao, 1996) accounts for moderately large deflections, where the deflection is assumed to be of the same order of magnitude as the strip slenderness ratio  $\tau/L$ , and non-negligible normal stress variation in the lateral (axial) direction. In GB, with zero axial loading present, the deflection of the floating beam over shallow water is given by,

$$m\partial_t^2 \eta - I_r \partial_t^2 \partial_x^2 \eta + D\partial_x^4 \eta - s(\partial_x \eta)^2 \partial_x^2 \eta + \rho_w g \eta + \rho_w \partial_t \phi + \frac{\rho_w}{2} (\partial_x \phi)^2 = -q(x, t)$$
 (5)

In addition to the inertial and bending rigidity terms, which are similar to EB, rotary inertia effects are accounted through the term  $-I_r\partial_t^2\partial_x^2\eta$ , where  $I_r$  is the rotary stiffness coefficient. The nonlinear term  $-s(\partial_x\eta)^2\partial_x^2\eta$ , with  $s=3E\tau(1-v^2)^{-1}/2$ , is a product of the large deflection assumption, where up to second order strain terms are kept in the Green-St. Venant strain tensor.

## 2.1 Initial Boundary Value problems

In the following section, the IBV problems of a freely-floating nonlinear strip, interacting with a surface wave propagating in a shallow water environment, modeled first by the linearized and then by the full shallow water equations, are formulated.

The horizontal velocity vanishes at infinity, hence it holds

$$\partial_{\nu}\phi_{1}(|x| \to \infty, t) = \partial_{\nu}\phi_{2}(|x| \to \infty, t) = 0 \tag{6}$$

The unconstrained floating body configuration results in vanishing conditions for the shear stress and bending moments at the beam edges,

$$M_b(0,t) = V(0,t) = M_b(1,t) = V(1,t) = 0 \ t \in (0,T]$$
 (7)

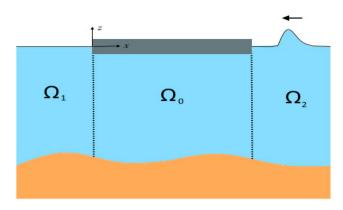


Figure 1 1D hydroelastic domain configuration

Introducing the non-dimensional quantities  $\tilde{x} = L^{-1}x$ ,  $\tilde{t} = g^{1/2}L^{-1/2}t$ ,  $\tilde{\eta} = L^{-1}\eta$  and  $\tilde{\phi} = g^{-1/2}L^{-3/2}\phi$ , and considering the corresponding non dimensional forms of the equations (1)-(5), two IBVPs can be defined. The problem defined by the weekly nonlinear GB-LSW model is given as,

$$\partial_t^2 \phi_1 - \partial_x (B(x)\partial_x \phi_1) = 0 \quad \text{in } \Omega_1, \tag{8}$$

$$\begin{split} M \varepsilon \partial_{t}^{2} \eta_{0} - I_{R} \varepsilon^{3} \partial_{t}^{2} \partial_{x}^{2} \eta_{0} + \varepsilon^{3} K \partial_{x}^{4} \eta_{0} - \varepsilon S (\partial_{x} \eta_{0})^{2} \partial_{x}^{2} \eta_{0} \\ + \eta_{0} + \partial_{t} \phi_{0} + Q(x, t) \end{split} \tag{9a}$$

$$\partial_t \eta + \partial_x \left( B(x) \partial_x \phi_0 \right) = 0 \quad \text{in } \Omega_0 , \tag{9b}$$

$$\partial_t^2 \phi_2 - \partial_x (B(x)\partial_x \phi_2) = 0 \text{ in } \Omega_2.$$
 (10)

with 
$$\eta_i = -\partial_t \phi_i$$
,  $i = 1, 2$ ,  $M = \rho_e / \rho_w$ ,  $B(x) = L^{-1}b(x)$ ,  $\varepsilon = \tau / L \ll 1$  and  $Q(x,t) = -q(x,t) \left(\rho_w g L\right)^{-1}$ .

At the interfaces, appropriate mass and momentum conservation conditions are expressed as

$$B(0^{-})\partial_{x}\phi_{1}\big|_{x=0^{-}} = B(0^{+})\partial_{x}\phi_{0}\big|_{x=0^{+}}, \partial_{t}\phi_{1}\big|_{x=0^{-}} = \partial_{t}\phi_{0}\big|_{x=0^{+}}, t \in (0,T]$$
(11a)

$$B(1^{-}) \partial_{x} \phi_{0} \Big|_{x=1^{-}} = B(1^{+}) \partial_{x} \phi_{2} \Big|_{x=1^{+}}, \partial_{t} \phi_{0} \Big|_{x=1^{-}} = \partial_{t} \phi_{2} \Big|_{x=1^{+}} t \in (0,T]$$

$$(11b)$$

Finally, the GB-SW hydroelastic model, where nonlinear terms are included in both hydrodynamic and elasticity models constitutes the following IBV problem,

$$\partial_t^2 \phi_1 + 2^{-1} \partial_t \left( \partial_x \phi_1 \right)^2 - \partial_x \left( B(x) \partial_x \phi_1 \right) + \frac{1}{2} \partial_x \left( \partial_x \phi_1 \right)^3 + \partial_x \left( \partial_t \phi_1 \partial_x \phi_1 \right) = 0 , \text{ in } \Omega_1$$
 (12)

$$\begin{split} M \mathcal{E} \partial_t^2 \eta_0 - I_R \mathcal{E}^3 \partial_t^2 \partial_x^2 \eta_0 + \mathcal{E}^3 K \partial_x^4 \eta_0 - \mathcal{E} S (\partial_x \eta_0)^2 \partial_x^2 \eta_0 \\ + \eta_0 + \partial_t \phi_0 + \frac{1}{2} (\partial_x \phi_0)^2 = Q(x, t) \end{split} \tag{13a}$$

$$\partial_t \eta + \partial_x ([B(x) + \eta_0] \partial_x \phi_0) = 0$$
, in  $\Omega_0$ , (13b)

$$\partial_{t}^{2}\phi_{2} + \frac{1}{2}\partial_{t}\left(\partial_{x}\phi_{2}\right)^{2} - \partial_{x}\left(B(x)\partial_{x}\phi_{2}\right) + \frac{1}{2}\partial_{x}\left(\partial_{x}\phi_{2}\right)^{3} + \partial_{x}\left(\partial_{t}\phi_{2}\partial_{x}\phi_{2}\right) = 0 \text{, in } \Omega_{2}. \tag{14}$$

$$\text{with } \eta_i = -\partial_t \phi_i - \frac{1}{2} \left( \partial_x \phi_i \right)^2 \ , \ i = 1, 2 \ , \ I_R = \frac{\rho_e}{12 \rho_w} \ , \\ S = \frac{3E}{2(1-v^2)\rho_w gL} \ \text{and} \ K = \frac{E(1-v)}{12(1+v)(1-2v)\rho_w gL} \ .$$

The interface conditions (11) are reformulated as

$$\left(B(0^{-}) + \eta_{1}(0^{-},t)\right) \partial_{x} \phi_{1} \Big|_{x=0^{-}} = \left(B(0^{+}) + \eta_{0}(0^{+},t)\right) \partial_{x} \phi_{0} \Big|_{x=0^{+}} \partial_{t} \phi_{1} \Big|_{x=0^{-}} = \partial_{t} \phi_{0} \Big|_{x=0^{+}}$$
(15a)

$$\left(B(1^{-}) + \eta_{0}(1^{-}, t)\right) \partial_{x} \phi_{0} \Big|_{x=1^{-}} = \left(B(1^{+}) + \eta_{2}(1^{+}, t)\right) \partial_{x} \phi_{2} \Big|_{x=1^{+}} \partial_{t} \phi_{0} \Big|_{x=1^{-}} = \partial_{t} \phi_{2} \Big|_{x=1^{+}}$$
(15b)

Initially the plate and fluid are assumed to be at rest while an upper surface elevation is imposed at the right half strip, corresponding to the following initial conditions

$$\eta_0(x,0) = \phi_0(x,0) = 0 \text{ in } \Omega_0, \quad \phi_1(x,0) = \partial_t \phi_1(x,0) = 0 \text{ in } \Omega_1 \text{ and}$$

$$\phi_2(x,0) = 0, \quad \partial_t \phi_2(x,0) = -G(x) \text{ in } \Omega_2$$
(16)

where G(x) is an upper surface elevation imposed in subregion  $\Omega_2$ .

#### 3 Variational formulation

In the present section, the equivalent variational formulations of the IBVPs defined previously will be presented. First, the systems of Eqs. (8) - (10) and (12)-(14) are multiplied by the weight functions  $w_1 \in H^1(\Omega_1)$ ,  $v \in H^2(\Omega_0)$  and  $w_2 \in H^1(\Omega_2)$  accordingly. Then, performing integration by parts, adding the corresponding equations and applying the appropriate interface and farfield conditions, yields the following variational problem,

Find  $\eta_0$  and  $\phi_i$ , i = 0,1,2, such that for every  $w_i \in H^1(\Omega_i)$ , i = 0,1,2 and  $v \in H^2(\Omega_0)$  it is

$$\int_{-\infty}^{0} \left[ w_{1} \partial_{t}^{2} \phi_{1} + \lambda w_{1} \partial_{x} \phi_{1} \partial_{tx}^{2} \phi_{1} + \partial_{x} w_{1} B(x) \partial_{x} \phi_{1} - \frac{\lambda}{2} \partial_{x} w_{1} \left( \partial_{x} \phi_{1} \right)^{3} - \lambda \partial_{x} w_{1} \partial_{t} \phi_{1} \partial_{x} \phi_{1} \right] dx 
+ \int_{0}^{1} \left[ M \varepsilon v \partial_{t}^{2} \eta_{0} + I_{R} \varepsilon^{3} \mu \partial_{x} v \partial_{t}^{2} \partial_{x} \eta_{0} + \varepsilon^{3} K \partial_{x}^{2} v \partial_{x}^{2} \eta_{0} + \frac{\varepsilon S \mu}{3} \partial_{x} v (\partial_{x} \eta_{0})^{3} \right] dx 
+ \int_{0}^{1} \left[ v \eta_{0} + v \partial_{t} \phi_{0} + \frac{\mu}{2} v \left( \partial_{x} \phi_{0} \right)^{2} - w_{0} \partial_{t} \eta_{0} + \partial_{x} w_{0} [B(x) + \lambda \eta_{0}] \partial_{x} \phi_{0} \right] dx 
+ \int_{1}^{+\infty} \left[ w_{2} \partial_{t}^{2} \phi_{2} + \lambda w_{2} \partial_{x} \phi_{2} \partial_{tx}^{2} \phi_{2} + \partial_{x} w_{2} B(x) \partial_{x} \phi_{2} - \frac{\lambda}{2} \partial_{x} w_{2} \left( \partial_{x} \phi_{2} \right)^{3} - \lambda \partial_{x} w_{2} \partial_{t} \phi_{2} \partial_{x} \phi_{2} \right] dx 
= \int_{0}^{1} v Q(x, t) dx, \quad \mu, \lambda = 0, 1$$

 $\begin{array}{l} \textit{and} \quad (\phi_1(x,0),w_1)_1 = (\phi_0(x,0),w_0)_0 = (\phi_2(x,0),w_2)_2 = 0 \quad , \quad (\eta_0(x,0),w_0)_0 = (\partial_t\phi_1(x,0),w_1)_1 = 0 \quad , \\ \left(\partial_t\phi_2(x,0),w_2\right)_2 = -\left(G(x),w_2\right)_2 \text{ , with } (\ ,\ )_i \ , \ i = 0,1,2 \text{ being the } L^2 \text{ -inner product in region } \Omega_i \, . \end{array}$ 

Setting  $\lambda=0$  and  $\mu=1$  retrieves the variational formulation of the GB-LSW IBV problem, while setting  $\lambda=1$  and  $\mu=1$  results in the variational equivalent of the GB-SWE IBV problem. Notably, setting  $\lambda=0$   $\mu=0$ , Eq. (17) reduces to the variational equivalent of the linear hydroelastic problem formulated by means of the EB-LSW model.

#### 3.1 Finite element formulation

Next, the finite element method will be employed for the numerical solution of the variational problem described by Eq. (17). The velocity potential of the free water surface regions are approximated by quadratic Lagrange elements while a special, 5-node element is introduced for the hydroelasticity dominated region. The reader is directed to the work of Papathanasiou *et al.* (2015 (b)) for a more in depth analysis. The hydroelastic element incorporates  $5^{th}$  order Hermite polynomials for the interpolation of the beam deflection/upper surface elevation in the middle region and  $4^{th}$  order Lagrange polynomials for the interpolation of the velocity potential. Hence the approximate solutions are taken as,  $\eta^h = \sum_{i=1}^6 H_i(x) \eta_i^h(t)$  for the middle region and  $\varphi_j^h = \sum_{i=1}^5 L_i(x) \varphi_{ij}^h(t)$ , j=1,2 for the free water surface regions. A second order system of ordinary differential equation is derived when the approximate solutions are substituted into a discretized Eq. (17). In the weakly nonlinear GB-LSW model case, the system is given as  $\mathbf{M}\ddot{u} + \mathbf{C}\dot{u} + \mathbf{K}(u)u = 0$ , where u is the vector of the nodal unknowns, while a system of the form  $\mathbf{M}\ddot{u} + \mathbf{C}(u)\dot{u} + \mathbf{K}(u)u = 0$  is produced by the GB-SW model. After setting  $\dot{u} = y$  and taking  $\mathbf{z} = [u\ y]^T$ , the previous is reduced to the first order system of nonlinear equations,  $\mathbf{A}\dot{z} + \mathbf{B}(z)z = 0$ . This last equation is integrated in time using a Crank-Nicolson time marching scheme.

#### 4 Numerical Results

In the present section, the three hydroelastic models are compared in a numerical example featuring variable bathymetry (see Figure 2). An incoming elevation pulse, typical in long wave modeling (Tadepalli & Synolakis, 1996), provides the initial excitation. Since the scope of the present work is to give a preliminary assessment of the accounted nonlinear effects, a single slenderness ratio  $\varepsilon = \tau / L$  for the floating body is investigated. The wavelength for both examined excitation scenarios is set at  $W = 300 \, m$  and the amplitude is taken as A = 0.4 and  $0.8 \, m$ , thus the examined wave steepness ratios are set to A/W = 0.0013 and 0.0027.

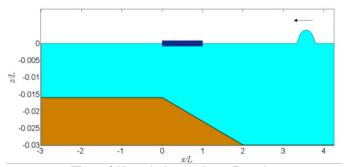


Figure 2 Numerical example configuration

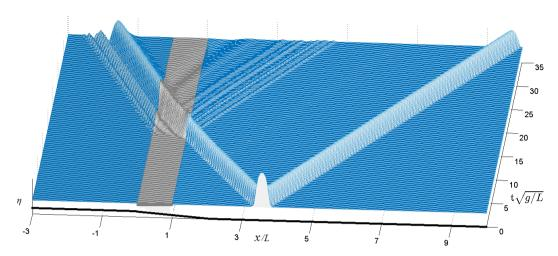
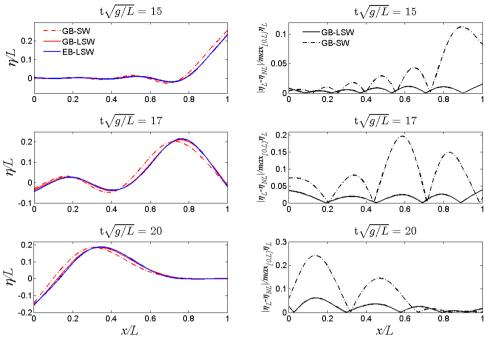


Figure 3 Space time plot of the elevation pulse propagation

The incoming forcing initially transverses over a flat bottom, set at a depth of 15 m, until it reaches a shoaling region where the depth is assumed to decrease linearly to 8 m, where it is kept constant (Figure 2). The strip is assumed to be floating over the shoaling region. The uniform thickness of the body is set at  $\tau = 3m$ , while its length was taken as L = 500m, resulting in a slenderness ratio of  $\varepsilon = 0.006$ . Finally, the material constants selected are; density  $\rho_e = 922.5 \ kg / m^3$ , water density  $\rho_w = 1025 \ kg / m^3$ , Young's modulus  $E = 5 \cdot 10^9 \ Pa$  and Poisson's ratio v = 0.3.

For the given analysis, 150 special hydroelastic elements and 10000 time steps were employed for the approximation of the middle region and the calculation of the transient strip response. In Figure 3 a space time plot illustrating the propagation of the imposed upper surface elevation in  $\Omega_2$  is shown. The initial pulse in split into two propagating waves, travelling in opposite directions. As the wave travelling towards the negative x-axis reaches the shoaling region it is partially reflected. When the wave impacts the free edge of the floating strip, the hydroelastic pulse begins to propagate showing dispersive characteristics. A reflected wave back propagating in  $\Omega_2$  is formed at impact.

In Figure 4 and Figure 5, the solutions obtained by means of the fully linear (EB-LSW) and the two non-linear models are compared. The comparison is shown at three distinct moments in time representing the phases of wave impact, hydroelastic wave propagation and wave exit from the middle region. On the left column of the figures, the calculated strip responses are shown, while on the right the corresponding deviations from the linear model solution are presented. It is observed that the nonlinearity introduced by the GB-LSW is rather weak, since the strip response is essentially reduced to the EB-LSW solution for the examined excitation scenarios. The deviation between the GB-LSW and the EB-LSW models is kept under 10% in both cases. Moreover, the deviation increase with increasing excitation steepness is minimal. This is attributed to the fact that the floating strip is considered thin in this case. Since,  $\varepsilon \ll 1$ , the rotary inertia and nonlinear terms of the Gao beam model are rather weak (see Eq 9(a)) and the solution is reduced to the one calculated by the classical thin beam theory. The limitations posed by the linear model would become evident with increasing dimensionless parameter  $\varepsilon$ . On the other hand, the deviations between the GB-SW and the EB-LSW solutions seem to increase proportionally with excitation steepness. In Figure 4 the maximum deviation is seen to exceed 20 % while in Figure 5 it exceeds 40%. Hence, the nonlinearity introduced in the hydrodynamic modeling is dominant over the nonlinear effects incorporated by the large deflections assumption of the strip model.



**Figure 4** (**Left**)Strip response at given moments in time, calculated by the EB-LSW , GB-LSW and GB-SW models for an elevation pulse with a steepness ratio of 0.0013.(**Right**) Deviations between the calculated solutions by the GB-LSW and GB-SW models and the fully linear EB-LSW model.

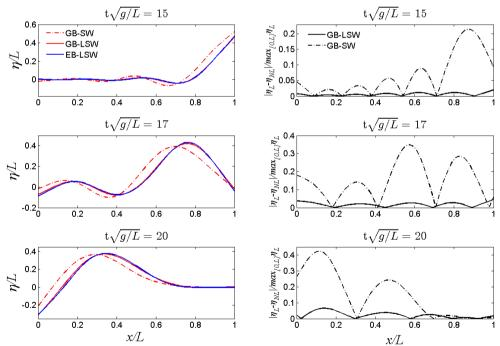


**Figure 5** (**Left**)Strip response at given moments in time, calculated by the EB-LSW , GB-LSW and GB-SW models for an elevation pulse with a steepness ratio of 0.0027.(. (**Right**) Deviations between the calculated solutions by the GB-LSW and GB-SW models and the fully linear EB-LSW model.

#### 5 Conclusions

In this contribution, a higher-order finite element scheme is employed for the solution of the 1D hydroelastic problem of a floating nonlinear strip in shallow water conditions. Two nonlinear hydroelastic models were considered. The Gao nonlinear beam is initially coupled with the linearized shallow water equations (GB-LSW model) and subsequently with the full nonlinear equations (GB-SW mode). The variational equivalent of the defined IBV problems were solved by mains a special 5-node hydroelastic element, featuring 5<sup>th</sup> order Hermite polynomials for the interpolation of the upper surface elevation/strip deflection in the middle region, and 4<sup>th</sup> order Lagrange polynomials for the interpolation of the velocity potential function in the same region. The higher-order finite element scheme was first applied in the solution of the hydroelastic problem of a floating, linear, elastic strip under the classical beam theory assumptions in Papathanasiou *et al.* (2015 (b)) and is now extended to nonlinear strip modeling.

In the present work, the nonlinear effects incorporated by the GB-LSW and GB-SW models were examined for a given floating body slenderness ratio and varying excitation steepness. When compared with the aforementioned linear model, the deviation between the calculated GB-SW and EB-LSW model solutions increases proportionally with increasing initial excitation steepness. In the case of the GB-LSW, the obtained strip responses under the examined excitations were essentially reduced to the ones calculated by the fully linear model, with the deviation between the solutions being kept under 10%. Hence, the nonlinearity in the hydrodynamic equations appeared to be dominant over the nonlinear effects introduced by the large deflections assumption in the strip model, for the examined non-dimensional slenderness parameter  $\varepsilon$ .

The present contribution is a first step in the implementation of higher-order finite element schemes in the solution of the hydroelastic problem with incorporated nonlinearity. Although the presented results give a clear indication of the strength of the accounted nonlinear effects, further investigation is required in order to establish the range of validity for the presented nonlinear hydroelastic models. Possible future extensions include the study of higher order shallow water wave and plate models in a general bathymetry.

## Acknowledgements

The author gratefully acknowledges Prof K. A. Belibassakis and Dr T. K. Papathanasiou for their valuable suggestions and constructive comments on the present work.

## References

- Athanassoulis, G. A., & Belibassakis, K. A. (1999). A consistent couple-mode theory for the propagations of small-amplitude water waves over variable bathymetry. *J. Fluid Mech.*, 389, 275-301.
- Belibassakis, K. A., & Athanassoulis, G. A. (2005). A coupled-mode model for the hydroelastic analysis of large floating bodies over bathymetry regions. *J. Fluid Mech.*, 531(221-249).
- Belibassakis, K. A., & Athanassoulis, G. A. (2006). A coupled-mode technique for weakly non-liner wave interaction with large floating bodies lying over variable bathymetry regions. *App. Ocean Res.*, 28, 59-76.
- Chen, X. J., Juncher Jensen, J., Cui, W. C., & Fu, S. X. (2003). Hydroelasticity of a floating plate in multidirectional waves. *Ocean Eng.*, 30(15), 1997-2017.

- Chen, X. J., Wu, Y. S., Cui, W. C., & Juncher Jensen, J. (2006). Review of hydroelasticity theories for global response of marine structures. *Ocean Eng.* (33), 439-457.
- Gao, D. Y. (1996). Nonlinear beam theory with applications to contact problems and variational approaches. *Mech. Res. Commun*, 11-17.
- Hegarty, G. M., & Squire, V. A. (2004). On Modelling the Interaction of Large Amplitude Waves with a Solitary Floe. *Proceedings of the Fourteenth International Offshore and Polar Engineering Conference*. Toulon, France.
- Meylan, M. H., & Squire, V. A. (1994). The response of ice floes to ocean waves. *J. Geophys. Res.*, 99, 891-900.
- Papathanasiou, T. K., Karperaki, A. E., Theotokoglou, E. E., & Belibassakis, K. A. (2015 (a)). Hydroelastic analysis of ice shaleves under long wave excitation. *Nat. Hazards Earth Syst. Sci.*, 15, 1-7.
- Papathanasiou, T., Karperaki, A., Theotokoglou, E. E., & Belibassakis, K. A. (2015 (b)). A higher order FEM for time-domain hydroelastic analysis of large floating structures in an inhomogeneouw shallow water environment. *Proc. R. Soc. A*, 471.
- Squire, V. A. (2008). Synergies between VLFS Hydroelasticity and Sea Ice Research. *Int. J. Offshore Polar Eng.*, 18(3), 1-13.
- Sturova, I. V., A., K. A., Fedotova, Z. I., Chubarov, L. B., & Komarov, V. A. (2010). Nonlinear dynamics of non-uniform elastic plate floating on shallow water of variable depth. *5th International Comnference on Hydroelasticity*. Southampton, UK.
- Tadepalli, S., & Synolakis, K. (1996). Model for the leading waves of tsunamis. *Phys. Rev. Lett.*, 77, 2141-2144.
- Wang, C. M., Watanabe, E., & Utsunomiya, T. (2008). Very large floating structures. London: Taylor and Francis.